triethylenetetramine, 112-24-3; methyl salicylate, 119-36-8; 1,10-diamino-4,7-diazadecane, 10563-26-5.

Supplementary Material Available: Listings of anisotropic thermal parameters (Tables VII and VIII), complete bond distances (Tables IX and X) and angles (Tables XI and XII), and hydrogen atom positional parameters (Tables XIII and XIV) for $MnL^2 \cdot 4H_2O$ and $MnL^3 \cdot MeOH$ (7 pages); listings of observed and calculated structure factors for the above two complexes (23 pages). Ordering information is given on any current masthead page.

Contribution from the Dipartimento di Chimica Generale, Università di Pavia, 27100 Pavia, Italy

Using Platinum(II) as a Building Block to Two-Electron Redox Systems. Crystal Structure and Redox Behavior of *cis*-[Pt^{II}(3-ferrocenylpyridine)$_2Cl_2$]

Oliviero Carugo, Giancarlo De Santis, Luigi Fabbrizzi,* Maurizio Licchelli, Alberto Monichino, and Piersandro Pallavicini

Received June 13, 1991

Reaction of 3-ferrocenylpyridine (3-FcPy) with $[Pt^{II}Cl_4]^{2-}$ gave the square complex *cis*-[Pt^{II}(3-FcPy)$_2Cl_2$], which was structurally characterized by X-ray crystallography. The compound, $C_{33}H_{32}Cl_2Fe_2N_2OPt$, containing a disordered acetone molecule, crystallizes in the triclinic $P\bar{1}$ space group, with unit cell parameters a = 9.976 (9) Å, b = 10.53 (1) Å, c = 16.89 (1) Å, α = 106.5 (1)°, β = 97.8 (1)°, γ = 102.8 (1)°, V = 1621 (6) Å^3, Z = 2, and d(calcd) = 1.742 g cm^{-3}. The structure converged to an R factor of 3.5%. *cis*-[Pt^{II}(3-FcPy)$_2Cl_2$], in acetone, DMSO, or MeCN solution, undergoes a two-electron oxidation process, according to two one-electron reversible steps, which involve the two appended ferrocenyl fragments, whose potentials are separated by only the statistical term (36 mV). It is demonstrated that the *cis*-[py_2Pt^{II}] core is a convenient bridging unit to build up novel bis(ferrocene) systems, in which the two relatively close Fc fragments display independent redox activity.

Introduction

Ferrocene is one of the most classical redox agents of organometallic chemistry. Its tendency to undergo a one-electron oxidation process to give the stable ferrocenium ion was demonstrated since its very first appearance on the chemical stage.[1] The ferrocene/ferrocenium (Fc/Fc^+) redox change is so clean and reversible from an electrochemical point of view that ferrocene is more and more frequently used as an internal standard for voltammetric investigations in nonaqueous and poorly polar solvents: ferrocene is dissolved in solution in the same concentration as the investigated electroactive species, and the potential scale is calibrated versus the reversible wave associated with the oxidation of ferrocene. Thus, the Fc^+/Fc couple is now being widely accepted as the nonaqueous counterpart of SHE (or SCE).[2]

Moreover, the ferrocene subunit has been used as a fragment for the design of multielectron redox systems. In particular, bridging two ferrocene subunits generates a redox agent able to exchange a couple of electrons according to two reversible one-electron steps. The mode of the two-electron release by the Fc–R–Fc system (the electron may be exchanged (i) at the same potential or (ii) through two distinct and well-defined steps) depends upon the nature of the bridging fragment R. Bridging of ferrocenyl fragments has been classically carried out by means of carbon chains of varying length and nature: the linking segment may or may not allow communication between the ferrocenyl subunits, influencing the mode of the two-electron release.[3] More recently, Wrighton synthesized 4-ferrocenylpyridine (**1**, 4-FcPy),

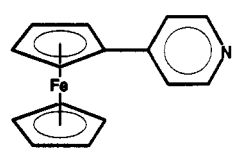

1

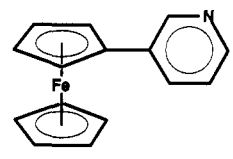

2

which has been designed as a ligand containing a pendant redox active unit. Reaction of 4-FcPy with $Re(CO)_5Cl$ gave the Re-(4-FcPy)$_2$(CO)$_3$Cl complex.[4] This species has an octahedral stereochemistry, and the two 4-FcPy molecules occupy adjacent coordination sites, as indicated by the identical NMR parameters of the two pyridine ligands. *fac*-(4-FcPy)$_2$(CO)$_3$Cl, which was designed with the aim to modulate the spectroscopic properties of the metal center (Re) by changing the oxidation state of the peripheral Fc subunits, represents a novel example of bis(ferrocene), in which the bridging unit is a transition-metal coordination compound: e.g. the *cis*-Py_2Re^+ core. It should be noted that using bridging segments derived from organic chemistry gives angles of 109, 120, and 180°, according to the type of hybridization of the carbon atom(s). The novelty of using transition-metal centers as bridging segments is that the envisaged redox units (e.g. Fc) can be situated at different angles.

We wished to further explore this possibility by binding two ferrocenylpyridine molecules to a transition-metal center prone to a cis type of coordination. In particular, we used 3-ferrocenylpyridine (**2**, 3-FcPy), which can be conveniently obtained through a *one-pot* synthesis, which involves diazo coupling of ferrocene and pyridine. Reaction of 3-FcPy with $[Pt^{II}Cl_4]^{2-}$ gave the *cis*-[Pt^{II}(3-FcPy)$_2Cl_2$] complex. Pt^{II} was chosen as a metal center as it gives with ligands containing nitrogen donor atoms complexes which are very stable from both a thermodynamic and a kinetic point of view. Due to its preferred cis mode of coordination, Pt^{II} as a bridging segment should be able to place the two ferrocene subunits along two planes which form an angle different from those generally obtained by using segments derived from organic chemistry. This work describes the crystal and molecular structure of *cis*-[Pt^{II}(3-FcPy)$_2Cl_2$] as well as its solution behavior, with a special regard to the two-electron oxidation process to give *cis*-[Pt^{II}(3-FcPy$^+$)$_2Cl_2$]$^{2+}$.

Experimental Section

Ferrocene (Fluka) was recrystallized from hexane. All other reagents and starting materials used in the synthetic work were used as received. ^{1}H NMR spectra (solvent $CDCl_3$, internal TMS standard) were measured on 80- or 300-MHz Bruker instruments. UV–vis spectra were recorded on a Hewlett-Packard 8452 diode-array spectrometer.

3-Ferrocenylpyridine (3-FcPy) (2). Synthesis of the ligand was performed by using a modification of the literature method.[5] 3-Aminopyridine (0.1 mol) was dissolved in aqueous 20% HCl (100 mL). To this

(1) Wilkinson, G.; Rosenblum, M.; Whiting, M. C.; Woodward, R. D. *J. Am. Chem. Soc.* **1952**, *74*, 2125.
(2) Gritzner, G.; Küta, J. *Pure Appl. Chem.* **1984**, *56*, 462 and references therein.
(3) Morrison, W. H., Jr.; Krogsrud, S.; Hendrickson, D. N. *Inorg. Chem.* **1973**, *12*, 1998.
(4) Miller, T. M.; Kazi, J. A.; Wrighton, M. S. *Inorg. Chem.* **1989**, *28*, 2347.
(5) Schlögl, K.; Fried, M. *Monatsh. Chem.* **1963**, *94*, 537.

0020-1669/92/1331-0765$03.00/0

Table I. Crystallographic Data for *cis*-$[Pt^{II}(3\text{-FcPy})_2Cl_2]$

empirical formula	$C_{33}H_{32}Cl_2Fe_2N_2OPt$	V, Å^3	1621 (6)
		Z	2
fw	850.32	d_{calcd}, g.cm^{-3}	1.742
specimen size, mm	0.31 × 0.28 × 0.20	radiation	Mo Kα (λ = 0.71069 Å) graphite monochromatized
space group	$P\bar{1}$		
a, Å	9.976 (9)		
b, Å	10.53 (1)	μ(Mo), cm^{-1}	54.171
c, Å	16.89 (1)	temp, deg	25
α, deg	106.5 (1)	R^a	0.035
β, deg	97.8 (1)	$R_w{}^b$	0.046
γ, deg	102.8 (1)		

$^a \sum||F_o| - |F_c||/\sum|F_o|$. $^b [\sum w(|F_o| - |F_c|)^2/\sum w|F_o|^2]^{1/2}$; w = unit weights.

ice-cooled solution was added a cold aqueous solution of $NaNO_2$ (0.11 mol in 20 mL of cold water) dropwise. Then, the diazonium salt solution was slowly added to a solution of ferrocene in CH_3COOH (0.052 mol in 500 mL). The resulting mixture was stirred for 4 h at room temperature and then poured into 500 mL of water. The brown mixture, made basic through the addition of aqueous 40% NaOH, was filtered off under vacuum, and the precipitate was collected. The dark brown solid was washed several times with Et_2O, while the orange aqueous solution was exhaustively extracted with Et_2O. The ethereal phases were collected, washed with water to neutrality, and dried over $MgSO_4$. The yellow-orange solution was concentrated by rotary evaporation to obtain a crude orange product containing unreacted ferrocene, 3-ferrocenylpyridine, and disubstituted ferrocene. The crude mixture was chromatographed on alumina by using a decreasing toluene/Et_2O ratio (from 9:1 to 1:1). 3-Ferrocenylpyridine was isolated in 32% yield from the second fraction (the first fraction was unreacted ferrocene) as orange platelets, mp 56–58 °C (lit.[5] mp 57–59 °C). Anal. Calcd for $C_{15}H_{13}NFe$: C, 68.47; H, 4.98; N, 5.32. Found: C, 68.15; H, 4.53; N, 5.44. ^{1}H NMR ($CDCl_3$, δ): 8.69 (d, 1 H), 8.37 (dd, 1 H), 7.67 (dt, 1 H), 7.17 (m, 1 H), 4.60 (t, 2 H), 4.30 (t, 2 H), 4.00 (s, 5 H).

***cis*-$[Pt^{II}(3\text{-FcPy})_2Cl_2]$ (3).** A solution of K_2PtCl_4 (0.5 mmol) in H_2O/EtOH (2:1, 10 mL) was added dropwise to a stirred solution of 3-ferrocenylpyridine (1 mmol) in EtOH (10 mL). The solution became cloudy and a yellow-orange precipitate began to form during the addition. The mixture was stirred at room temperature for 2 days. The precipitate was filtered off, washed with water and EtOH, and dried. More product was obtained by refrigerating the filtrate solution for some days. Total yield: 63%. The product was recrystallized from DMF/H_2O. Anal. Calcd for $C_{30}H_{26}Cl_2Fe_2N_2Pt$: C, 45.48; H, 3.31; N, 3.53. Found: C, 45.63; H, 3.23; N, 3.48. ^{1}H NMR ($CDCl$ δ): 8.92 (d, 1 H), 8.49 (dd, 1 H), 7.77 (dd, 1 H), 7.18 (m, 1 H), 4.61 (t, 2 H), 4.40 (t, 2 H), 4.00 (s, 5 H).

[*cis*-$[Pt^{II}(3\text{-}Fc^+Py)_2Cl_2]](ClO_4)_2$. A 5-mL aliquot of a CH_2Cl_2 solution 10^{-3} M in **3** was treated in a stoppered test tube with an equal volume of an aqueous Ce^{IV} solution (10^{-1} M in 1 M H_2SO_4). After vigorous shaking, the CH_2Cl_2 layer decolorized, while the aqueous phase took on a deep green color. On addition of some drops of 70% $HClO_4$ to the aqueous layer, a green precipitate formed. It was separated through filtration as a microcrystalline green solid, repeatedly washed with acetone, and dried in a stream of N_2. Anal. Calcd for $C_{30}H_{26}Cl_4Fe_2N_2O_8Pt$: C, 36.35; H, 2.64; N, 2.82. Found: C, 35.93; H, 2.78; N, 2.97.

X-ray Crystallography. Orange crystals of *cis*-$[Pt^{II}(3\text{-FcPy})_2Cl_2]$ suitable for the X-ray analysis were obtained by cooling in a refrigerator for several days a concentrated solution of the complex in acetone, to which a small amount of water had been added. Data were collected on a Philips PW 1100 four-circle diffractometer. Crystallographic data are given in Table I. Cell parameters were obtained by least-squares analysis of the θ angles of 25 reflections automatically centered in the range 10° < θ < 18°. The space group was determined on the basis of intensity statistics and confirmed by the structure refinement. A total of 5715 reflections, $\pm h,\pm k,+l$, were collected in the θ range 2–25° with scan mode $\omega/2\theta$, scan speed 4.5° min^{-1}, and scan width 1.5° (in ω). No intensity deterioration of standard reflection was detected. L_p and empirical absorption[6] corrections were applied (the range of the absorption correction factor was 1.00–1.32). The structure was solved by the Patterson and Fourier method.

All non-H atoms were refined anisotropically by full-matrix least-squares techniques (unit weights were used to keep $\sum w(\Delta F)^2$ uniform over ranges of (sin θ)/λ and $|F_o|$) by using 4807 reflections [$I > 3\sigma(I)$]. Atomic scattering factors with anomalous dispersion coefficients were taken from ref 7. Although all H atoms were found in the ΔF maps, their positional parameters were calculated (distance C–H = 1.00 Å; isotropic thermal parameters B fixed at 5.0 Å^2) and not refined. An acetone molecule, not interacting with the complex, is present in the crystal; as it has been impossible to completely refine the positional parameters of this acetone molecule, it is reasonable to suppose that it is highly disordered. The calculations were performed with the programs cited in ref 8. Table II reports the positional parameters of the non-H atoms.

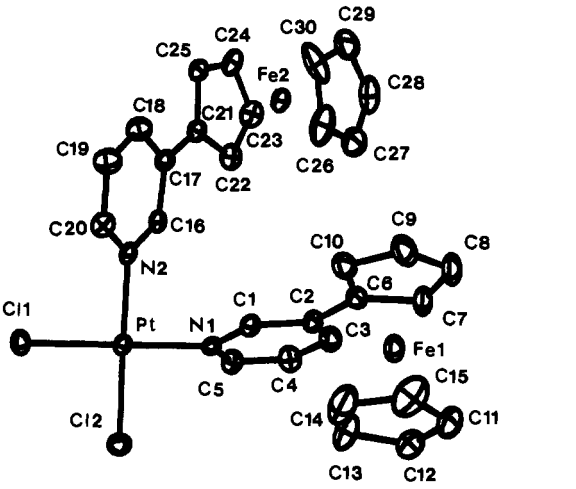

Figure 1. ORTEP view of *cis*-$[Pt^{II}(3\text{-FcPy})_2Cl_2]$ showing the atom-labeling scheme and 20% probability thermal ellipsoids.

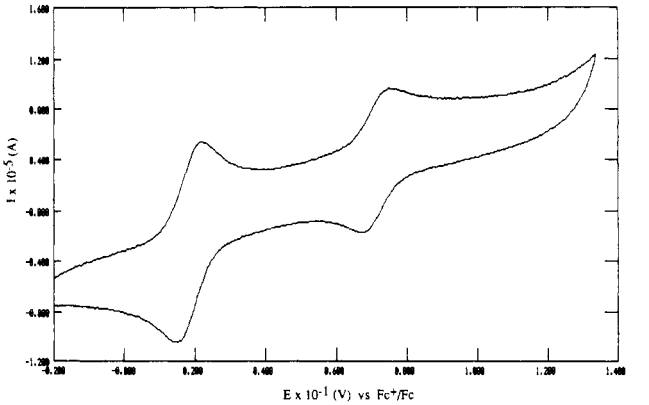

Figure 2. CV profile of a MeCN solution 5 × 10^{-4} M in *cis*-$[Pt^{II}(3\text{-FcPy})_2Cl_2]$ and 0.1 M in $[Bu_4N]ClO_4$ measured at 200 mV s^{-1}. The more anodic peak refers to the redox couple used as an internal reference: $[Fe^{III,II}(phen)_3]^{3+,2+}$. The scale of potential has been calibrated vs the Fc^+/Fc couple.

Electrochemistry. The solvents used in the electrochemical experiments (MeCN and DMSO) were distilled over CaH_2 and stored under nitrogen over molecular sieves. Acetone was dried over molecular sieves overnight prior to use. Supporting electrolyte, $[Bu_4N]ClO_4$ (Fluka, polarographic grade), was used without further purification. Electrochemical measurements (CV and DPV) were performed in a conventional three-electrode cell, using a PAR 273 potentiostat/galvanostat controlled by an IBM AT personal computer and driven by dedicated software. A silver wire was used as a pseudoreference electrode and was calibrated using $[Fe(phen)_3](ClO_4)_2$ as an internal standard. $[Fe^{II}(phen)_3](ClO_4)_2$ was chosen as the $E_{1/2}(Fc^+/Fc)$ value is too close to the potential values associated with the investigated redox changes. In a separate experiment, the potential associated with the $[Fe^{II,III}(phen)_3](ClO_4)_{2,3}$ redox change was measured vs the ferrocene/ferrocenium couple ($E_{1/2}$ = 0.703 V). Thus, all the potentials reported in this work have been referred to the classical Fc^+/Fc standard couple. Controlled-potential coulometry experiments were performed on MeCN solutions (5 × 10^{-4} M) using an Amel Mod. 563 apparatus and employing a platinum gauze as a working electrode.

(6) North, A. C. T.; Phillips, O. C.; Mathews, F. S. *Acta Crystallogr., Sect. A: Found Crystallogr.* **1968**, *A24*, 351.

(7) *International Tables for X-Ray Crystallography*; Kynoch Press: Birmingham, England, 1974; Vol. IV.

(8) Busing, W. R.; Martin, K. O.; Levy, H. A. ORFLS. Report ORNL-TM-305; Oak Ridge National Laboratory: Oak Ridge, TN 1963. SDP Enraf-Nonius program. Frenz, B. A. and Associates Inc., College Station, TX, and Enraf-Nonius, Delft, Holland, 1985.

Table II. Positional (Fractional Coordinates) and Thermal (Å^2) Parameters of Non-Hydrogen Atoms, with Esd's in Parentheses[a]

atom	x	y	z	B
Pt	0.2611 (1)	0.0028 (1)	0.4994 (1)	2.73 (1)
Fe(1)	0.5937 (1)	0.2856 (1)	0.8908 (1)	4.18 (1)
Fe(2)	0.0915 (1)	−0.4133 (1)	0.7309 (1)	3.63 (1)
Cl(1)	0.3056 (2)	−0.0756 (2)	0.3667 (1)	3.99 (1)
Cl(2)	0.2267 (2)	0.1991 (2)	0.4771 (2)	4.33 (1)
N(1)	0.2298 (6)	0.0719 (6)	0.6178 (4)	2.70 (1)
N(2)	0.2823 (6)	−0.1726 (6)	0.5216 (4)	2.75 (1)
C(1)	0.3288 (7)	0.0810 (8)	0.6839 (5)	3.07 (1)
C(2)	0.3081 (8)	0.1188 (8)	0.7668 (5)	3.44 (1)
C(3)	0.1797 (10)	0.1457 (10)	0.7784 (6)	4.48 (1)
C(4)	0.0816 (9)	0.1368 (10)	0.7108 (6)	4.34 (1)
C(5)	0.1081 (8)	0.0987 (9)	0.6313 (5)	3.78 (1)
C(6)	0.4161 (9)	0.1268 (8)	0.8365 (5)	3.72 (1)
C(7)	0.4221 (10)	0.1870 (10)	0.9242 (6)	0.487 (1)
C(8)	0.5432 (12)	0.1780 (12)	0.9713 (6)	5.75 (1)
C(9)	0.6146 (12)	0.1124 (12)	0.9159 (7)	5.96 (1)
C(10)	0.5397 (11)	0.0798 (10)	0.8325 (6)	5.01 (1)
C(11)	0.7012 (14)	0.4834 (12)	0.9593 (7)	6.72 (1)
C(12)	0.5878 (14)	0.4815 (12)	0.9008 (8)	6.72 (1)
C(13)	0.6052 (15)	0.4123 (13)	0.8213 (8)	7.70 (1)
C(14)	0.7270 (14)	0.3741 (14)	0.8291 (9)	8.67 (2)
C(15)	0.7872 (12)	0.4168 (15)	0.9174 (10)	8.38 (2)
C(16)	0.1825 (7)	−0.2388 (8)	0.5536 (4)	2.94 (1)
C(17)	0.1884 (8)	−0.3569 (8)	0.5723 (5)	3.16 (1)
C(18)	0.3024 (9)	−0.4095 (9)	0.5550 (6)	4.24 (1)
C(19)	0.4022 (9)	−0.3409 (10)	0.5218 (7)	4.70 (1)
C(20)	0.3910 (8)	−0.2229 (9)	0.5058 (5)	3.64 (1)
C(21)	0.0763 (8)	−0.4239 (8)	0.6076 (5)	3.27 (1)
C(22)	−0.0300 (9)	−0.3685 (10)	0.6416 (6)	4.25 (1)
C(23)	−0.1133 (9)	−0.4464 (11)	0.6690 (6)	4.52 (1)
C(24)	−0.0621 (10)	−0.5809 (10)	0.6531 (6)	4.74 (1)
C(25)	0.0561 (9)	−0.5566 (8)	0.6160 (5)	3.84 (1)
C(26)	0.2731 (13)	−0.2764 (16)	0.8005 (8)	8.00 (2)
C(27)	0.1700 (16)	−0.2431 (13)	0.8348 (8)	7.54 (2)
C(28)	0.1016 (13)	−0.3476 (16)	0.8577 (7)	7.53 (1)
C(29)	0.1625 (18)	−0.4539 (14)	0.8359 (8)	8.16 (1)
C(30)	0.2733 (15)	−0.4089 (20)	0.7987 (8)	9.19 (2)
O(1)	0.0963 (27)	0.0203 (27)	0.1624 (19)	15.93 (4)
C(31)	0.2234 (33)	0.1421 (38)	0.1966 (20)	9.25 (1)
C(32)	0.2510 (32)	0.1944 (24)	0.1193 (19)	8.68 (1)
C(33)	0.3065 (45)	0.2084 (35)	0.2396 (34)	18.81 (5)

[a] Isotropic equivalent displacement parameters are defined as $^4/_3$-[$a^2B(1,1) + b^2B(2,2) + c^2B(3,3) + ab(\cos\gamma)B(1,2) + ac(\cos\beta)B(1,3) + bc(\cos\alpha)B(2,3)$].

Results

Description of the Structure. An ORTEP view of the *cis*-[Pt^{II}(3-FcPy)$_2Cl_2$] molecule is reported in Figure 1. Table III shows some selected bond distances and angles.

Electrochemical Studies. Voltammetry investigations on the *cis*-[Pt^{II}(3-FcPy)$_2Cl_2$] complex and the parent compounds were performed in acetonitrile solution, made 0.1 M in [Bu_4N]ClO_4. Cyclic voltammetry (CV) investigation at the platinum-microsphere working electrode disclosed an oxidation peak, followed by a reduction peak in the reverse scan. Figure 2 shows the CV profile, taken at a scan rate of 200 mV s^{-1}, for a solution 10^{-3} M in both *cis*-[Pt^{II}(3-FcPy)$_2Cl_2$] and [Fe^{II}(phen)$_3$]$(ClO_4)_2$, which was used as an internal reference. The ratio of the current intensity of the anodic peak over the intensity of the cathodic peak, i_a/i_c, was unity over the potential scan rate range 10–200 mV s^{-1}. $E_{1/2}$ was 0.170 V vs the Fc^+/Fc internal reference and the $E_a - E_c$ difference was 60 mV. On the other hand, using the differential pulse voltammetry (DPV) technique, and imposing a 10-mV pulse voltage, a symmetric peak centered at 0.170 V vs Fc^+/Fc was observed, whose half-peak width was 93 mV.[9] Then, the controlled-potential coulometry experiment was carried out on a MeCN solution 5×10^{-3} M in *cis*-[Pt^{II}(3-FcPy)$_2Cl_2$] and 0.1 M in [Bu_4N]ClO_4, imposing at the platinum-gauze working electrode a potential of 0.30 V vs Fc^+/Fc: 1.97 mol of electrons/mol of *cis*-[Pt^{II}(3-FcPy)$_2Cl_2$] complex were consumed during the electrolysis. The profile of the absorption spectrum in the UV–vis region of the blue-green electrolyzed solution is typical of a ferrocenium cation (see Figure 3). The oxidized complex *cis*-[Pt^{II}(3-Fc^+Py)$_2Cl_2$]$^{2+}$ is not indefinitely stable in MeCN solution, but slowly decomposes according to a first-order pattern ($t_{1/2}$ = 400 min), as monitored through the decay of the band at 684 nm, to restore 50% of the intact reduced complex and unidentified fragments.

Two-Phase Redox Processes. Oxidation processes under two-phase conditions were performed in stoppered test tubes containing 5 mL of CH_2Cl_2 solution 10^{-3} M in **3** and an equal volume of the oxidizing solution (10^{-1} M Fe^{III} in aqueous 1 M HCl or 10^{-1} M Ce^{IV} in aqueous 1 M H_2SO_4). The closed test tubes were vigorously shaken for a few minutes by an electromechanical stirrer. UV–vis spectra of the green aqueous layer were recorded. The presence of an intense band at 648 nm demonstrated that oxidation of the two ferrocene subunits of **3** had taken place. When the oxidation process was performed with 10^{-1} M Ce^{IV} in 1 M $HClO_4$, a green precipitate of *cis*-[Pt^{II}(3-Fc^+-Py)$_2Cl_2$]$(ClO_4)_2$ was obtained at the water/CH_2Cl_2 interface.

The reduction process involving the *cis*-[Pt^{II}(3-Fc^+-Py)$_2Cl_2$]$(ClO_4)_2$ complex was investigated under homogeneous conditions. In particular, *cis*-[Pt^{II}(3-Fc^+-Py)$_2Cl_2$]$(ClO_4)_2$ was dissolved in MeCN to obtain a 10^{-3} M solution. A 2-mL aliquot of this solution was transferred into a 10 mm quartz cuvette and titrated with small portions (0.02 mL) of a MeCN solution made 10^{-2} M in 2,5-di-*tert*-butylhydroquinone. Spectra were recorded after every addition, until the ferrocenium band at 684 nm dis-

Table III. Selected Bond Distances (Å) and Angles (deg) with Esd's in Parentheses

Pt–Cl(1)	2.299 (4)	Pt–N(1)	2.016 (7)
Pt–Cl(2)	2.292 (4)	Pt–N(2)	2.035 (7)
Fe(1)–C(6)	2.038 (8)	Fe(1)–C(11)	2.034 (11)
Fe(1)–C(7)	2.034 (11)	Fe(1)–C(12)	2.036 (13)
Fe(1)–C(8)	2.048 (13)	Fe(1)–C(13)	2.008 (15)
Fe(1)–C(9)	2.033 (14)	Fe(1)–C(14)	2.025 (17)
Fe(1)–C(10)	2.020 (10)	Fe(1)–C(15)	2.018 (12)
Fe(2)–C(21)	2.037 (9)	Fe(2)–C(26)	2.012 (12)
Fe(2)–C(22)	2.033 (11)	Fe(2)–C(27)	2.031 (11)
Fe(2)–C(23)	2.041 (9)	Fe(2)–C(28)	2.035 (12)
Fe(2)–C(24)	2.033 (9)	Fe(2)–C(29)	2.014 (15)
Fe(2)–C(25)	2.008 (8)	Fe(2)–C(30)	1.995 (15)
N(1)–Pt–N(2)	88.5 (4)	N(2)–Pt–Cl(1)	90.6 (3)
N(1)–Pt–Cl(1)	177.7 (5)	N(2)–Pt–Cl(2)	177.0 (5)
N(1)–Pt–Cl(2)	89.6 (4)	Cl(1)–Pt–Cl(2)	91.4 (3)

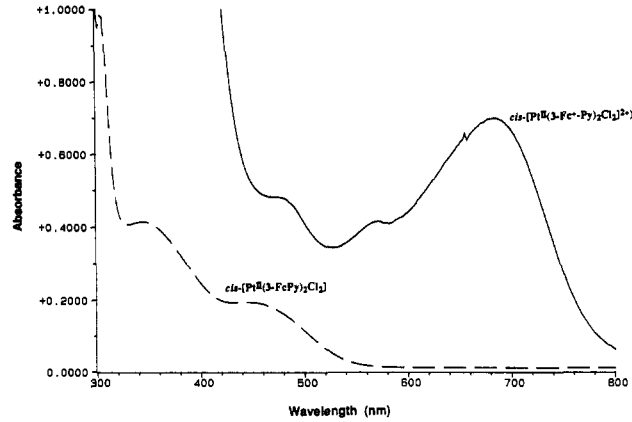

Figure 3. UV–vis spectra of MeCN solutions 10^{-3} M in *cis*-[Pt^{II}(3-FcPy)$_2Cl_2$] and {*cis*-[Pt^{II}(3-Fc^+Py)$_2Cl_2$]}$(ClO_4)_2$. The spectrum of the oxidized complex superimposes with that obtained for the diferrocenium cation anodically generated in MeCN 0.1 M in [Bu_4N]ClO_4.

(9) A peak separation of 57 mV (at 25 °C) in the CV profile corresponds to an electrochemically reversible one-electron process or to two one-electron consecutive reversible processes, whose potentials E_1 and E_2 are separated by 36 mV. A half-peak width of 90 mV in the DPV profile is expected for a reversible one-electron process or for a two-electron process in which $E_2 - E_1 = 36$ mV.[10]

(10) Richardson, D. E.; Taube, H. *Inorg. Chem.* **1981**, *20*, 1278.

appeared. At the end of titration, the solution was yellow and its spectrum was the same as that obtained from the *cis*-$[Pt^{II}(3\text{-}FcPy)_2Cl_2]$ solution. Homogeneous reduction of the oxidized complex was also performed with ascorbic acid, but in this case a 3:1 MeCN/water solution was used to increase the ascorbic acid solubility.

Discussion

Design of Ligands Carrying Independent Redox Activity. Ferrocenylpyridines represent a class of ligands carrying independent redox activity. Whereas the synthesis of 3- and 4-ferrocenylpyridine has been known for many years,[5] only recently have they been used as ligands carrying independent redox activity. The first example has been reported by Wrighton, who prepared 4-ferrocenylpyridine (**1**) by a different synthetic approach than ref 5 (i.e. through reaction of ferrocenylmagnesium bromide and 4-bromopyridine), and reacted it with $Re(CO)_5Cl$ to give the octahedral $(4\text{-}FcPy)_2(CO)_3Cl$ complex. We obtained 3-ferrocenylpyridine (**2**) through the coupling of diazo derivative of 3-aminopyridine (prepared in situ) and ferrocene, in acetic acid. The procedure is simple and convenient, as it involves the single-pot reaction of two commercially available and cheap reagents (3-aminopyridine and ferrocene, in the present case). The diazo-coupling procedure is a versatile and time-saving method to append ferrocenyl subunits to molecules of chosen coordinating tendencies, in order to prepare further ligands displaying independent redox activity. The condition is that the wanted molecule contains an anilino fragment prone to the formation of the diazo derivative. This procedure is currently being used in our laboratory to append ferrocene to classical ligands of transition metals: for instance, we recently obtained, through the diazo coupling method, ferrocenylsalycilate, which forms a stable 1:3 complex with Fe^{III}, displaying multielectron redox activity.[11]

Molecular Structure of *cis*-$[Pt^{II}(3\text{-}FcPy)_2Cl_2]$. The X-ray investigation confirmed that reaction of $[Pt^{II}Cl_4]^{2-}$ with 2 equiv of 3-FcPy gave the expected cis isomer. Formation of the trans isomer would require a totally different synthetic strategy. As far as the $[Pt^{II}(pyridine)Cl_2]$ core of the *cis*-$[Pt^{II}(3\text{-}FcPy)_2Cl_2]$ complex is concerned, no substantial differences are observed compared to the homologous *cis*-$[Pt^{II}(py)_2Cl_2]$ complex:[12] Pt^{II}–N distances lie in the 2.016 (7)–2.035 (7) Å range, and all the bond angles involving Pt^{II} exhibit the values expected for a regular square stereochemistry, 90.3 (2)°. The pyridine rings form angles of 58.2° [N(1), C(1)–C(5) ring] and 48.8° [N(2), C(16)–C(20) ring] with the square plane of the platinum complex. This arrangement is reminiscent of that observed in the *cis*-$[Pt^{II}(py)_2Cl_2]$ complex, where the angles formed between the pyridines and the coordination plane are 55.8 and 62°.[12] The angle between the planes containing the two pyridine rings is 66.1°, but each pyridine moiety is not coplanar with the cyclopentadienide ring to which is covalently bonded (the angles between the N(1) pyridine and the C(6) cyclopentadienide is 10.2°; that between the N(2) pyridine and the C(21) cyclopentadienide is 10.7°). As a consequence, cyclopentadienide rings of ferrocene subunits lie in two planes which form an angle of about 101°, so that ferrocenyl substituents are not oriented to be at the highest distance. Such a situation could be achieved by rotating one of the pyridine ring around the Pt^{II}–N axis. The reason of the chosen arrangement is not clear, at this stage of the investigation. However, it does not seem to generate any repulsive effect of steric origin, as indicated by the fact that no serious deviations or distortions are observed in the pertinent structural parameters and features ($NPt^{II}N$ angle, coplanarity of the bound pyridine–cyclopentadienide rings). As a consequence, the two Fe^{II} metal centers lie at a relatively short distance: 7.418 (2) Å. It is uncertain that present stereochemical arrangement, in particular as far as the relative positions of the appended ferrocenyl groups are concerned, is maintained in solution. In that case, the complex would present two equivalent redox active sites, the ferrocene subunits, at a moderate distance, in absence of any direct ring-to-ring bridge.

A final point is concerned with the conformation of the cyclopentadienide rings in each subunit. The conformation is in both subunits almost completely *eclipsed*. It has been pointed out that the energy difference between the two conformers is rather small[13] and the stability order may be altered through the introduction of substituents on the cyclopentadienide ring(s).

Redox Behavior of *cis*-$[Pt^{II}(3\text{-}FcPy)_2Cl_2]$. *cis*-$[Pt^{II}(3\text{-}FcPy)_2Cl_2]$ is not soluble in water, due to the presence of the hydrophobic ferrocenyl substituents, but it is fairly soluble in less polar solvents, such as acetonitrile (MeCN), dimethyl sulfoxide (DMSO), dimethylformamide (DMF), acetone, and dichloromethane. Cyclic voltammetry and controlled potential coulometry investigations have indicated that *cis*-$[Pt^{II}(3\text{-}FcPy)_2Cl_2]$ undergoes a two-electron oxidation process at the platinum electrode, according to the two consecutive one-electron steps

$$cis\text{-}[Pt^{II}(3\text{-}FcPy)_2Cl_2] = cis\text{-}[Pt^{II}(3\text{-}FcPy)(3\text{-}FcPy^{+})Cl_2]^{+} + e^{-} \quad (1)$$

$$cis\text{-}[Pt^{II}(3\text{-}FcPy)(3\text{-}FcPy^{+})Cl_2]^{+} = cis\text{-}[Pt^{II}(3\text{-}FcPy^{+})_2Cl_2]^{2+} + e^{-} \quad (2)$$

A peak separation of 57 mV in the CV response and a 90-mV half-peak width of the DPV profile, at 25 °C, are typical of a reversible one-electron process or a reversible *n*-electron process for a redox system containing *n* independent and noninterfering redox sites.[14] Thus, the release of two electrons by *cis*-$[Pt^{II}(3\text{-}FcPy)_2Cl_2]$ to the platinum electrode takes place through two one-electron steps that are controlled by the sole statistical term and whose potentials are separated by 36 mV. In other words, the comproportionation equilibrium (3), which results from the

$$cis\text{-}[Pt^{II}(3\text{-}FcPy)_2Cl_2] + cis\text{-}[Pt^{II}(3\text{-}FcPy^{+})_2Cl_2]^{2+} = 2\,cis\text{-}[Pt^{II}(3\text{-}FcPy)(3\text{-}FcPy^{+})Cl_2]^{+} \quad (3)$$

difference of eqs 1 and 2, is characterized by the statistical equilibrium constant $K = 4$. That means that the mixed-valence species *cis*-$[Pt^{II}(3\text{-}FcPy)(3\text{-}FcPy^{+})Cl_2]^{+}$ is not stabilized by any kind of electron delocalization, indicating that the Pt^{II} metal center prevents electron communication from a ferrocene moiety to the other one. Moreover, no repulsive electrostatic effects operate between the two redox sites. In principle, a mixed valence species of general formula A^{n+} is electrostatically stabilized with respect to the $A^{(n-1)+}$ and $A^{(n+1)+}$ forms only if $n > 1$.[10] Thus, if one considers the ferrocene fragment as definitely neutral ($n = 1$), equilibrium (3) should not profit at all from the electrostatic term. Moreover, the electrostatic advantage decreases with the increasing distance between the redox sites: thus, for a Fe–Fe distance such as that observed in the *cis*-$[Pt^{II}(3\text{-}FcPy)_2Cl_2]$ complex in the solid state, the electrostatic effect, if any, would disappear.

Table IV compares the E_1 and E_2 values pertinent to the *cis*-$[Pt^{II}(3\text{-}FcPy)_2Cl_2]$ complex with the $E_{1/2}$ value of the 3-FcPy molecule and that of ferrocene (the reference system, $E_{1/2} = 0$),

Table IV. Half-Wave Potential Values Associated with the One-Electron Oxidation of the Ferrocene Subunit in 3-Ferrocenylpyridine (3-Fcpy) and in the *cis*-$[Pt^{II}(3\text{-}FcPy)_2Cl_2]$ Complex, at 25 °C, in Selected Media (Made 0.1 M in $[Bu_4N]ClO_4$]) with $E_{1/2}$ Values (V) Referred to the Ferrocenium/Ferrocene (Fc^{+}/Fc) Couple

		MeCN	DMSO	acetone
3-FcPy		0.116	0.081	0.072
cis-$[Pt^{II}(3\text{-}FcPy)_2Cl_2]$	$E_{1/2}$	0.172	0.143	0.130
	E_1[a]	0.154	0.125	0.112
	E_2[a]	0.180	0.161	0.148

[a] E_1 and E_2 values refer to the processes involving each ferrocene subunit of the Pt^{II} complex. As the two-electron process is statistically controlled ($E_2 - E_1 = 36$ mV, at 25 °C), it follows that $E_1 = E_{1/2} - 0.018$ V and $E_2 = E_{1/2} + 0.018$ V.

(11) De Santis, G.; Fabbrizzi, L.; Licchelli, M.; Monichino, A.; Pallavicini, P.; Perotti, A. *Inorg. Chim. Acta* **1991**, *188*, 1.
(12) Colamarino, P.; Orioli, P. L. *J. Chem. Soc., Dalton Trans.* **1975**, *1656*.
(13) Cotton, F. A.; Wilkinson, G. *Advanced Inorganic Chemistry, 5th ed.*; Wiley: New York, 1988; p 79.
(14) Flanagan, J. B.; Margel, S.; Bard, A. J.; Anson, F. C. *J. Am. Chem. Soc.* **1978**, *100*, 4248.

in the same medium (MeCN, 0.1 M in $[Bu_4N]ClO_4$). The fact that the $E_{1/2}$ value observed with 3-FcPy is distinctly higher than that measured for Fc is to be ascribed to the electron-withdrawing effect exerted by the pyridine ring, which makes the removal of the electron from the ferrocene core more difficult. This electron-withdrawing effect is enhanced through coordination to the Pt^{II} metal center in the *cis*-[Pt^{II}(3-FcPy)$_2Cl_2$] complex (each 3-FcPy molecule being coordinated by $^1/_2$ Pt^{II}): in particular, coordination to the metal center raises the potential by about 50 mV. This effect is reasonable, considering that coordination further reduces the electron density on the nitrogen heteroatom. This behavior compares well with that observed for the (4-FcPy)$_2$Re(CO)$_3$Cl complex,[4] in which two electrons are released from the appended fragments, at the same potential, excluding the existence of any substantial electronic interaction between the ferrocene subunits.

The nature of the solvent does not affect the electrochemical behavior of the *cis*-[Pt^{II}(3-FcPy)$_2Cl_2$] complex: completely analogous responses have been observed in acetone and DMSO solutions, made 0.1 M in $[Bu_4N]ClO_4$, as documented by the data reported in Table IV.

If a dichloromethane layer containing *cis*-[Pt^{II}(3-FcPy)$_2Cl_2$] is equilibrated with an aqueous layer, the complex does not partition, but remains confined inside the nonaqueous phase. This is an interesting property which can be exploited to carry out redox process under two- or three-phase conditions. Design of multielectron redox systems to be used as carriers for the transport of electrons and ions across liquid membranes (a typical three-phase process) is currently being investigated in our laboratory. Thus, we tried preliminary two-phase oxidation experiments with *cis*-[Pt^{II}(3-FcPy)$_2Cl_2$] at the water/CH_2Cl_2 interface. However, equilibration of a 10^{-3} M CH_2Cl_2 solution of *cis*-[Pt^{II}(3-FcPy)$_2Cl_2$] with an equal volume of an aqueous solution containing oxidizing agents such as Fe^{III} (10^{-1} M, in 1 M HCl) or Ce^{IV} (10^{-1} M, in 1 M H_2SO_4) makes the aqueous layer turn blue-green. The band at 648 nm indicates that, due to the increased hydrophilicity, the diferrocenium cation, *cis*-[Pt^{II}(3-Fc^+-Py)$_2Cl_2$]$^{2+}$, partitions between the two phases. This prevents the use of the *cis*-[Pt^{II}(3-FcPy)$_2Cl_2$]/*cis*-[Pt^{II}(3-Fc^+Py)$_2Cl_2$]$^{2+}$ two-electron redox system as an electron carrier in liquid membrane transport experiments. If the *cis*-[Pt^{II}(3-FcPy)$_2Cl_2$]-containing CH_2Cl_2 layer is equilibrated with an aqueous layer 10^{-1} M in Ce^{IV} in 1 M $HClO_4$, a green precipitate forms at the interface. The same result is obtained if, after the two-phase oxidation process, the green aqueous phase is treated with $HClO_4$. The green solid analyzed as [Pt^{II}(3-Fc^+Py)$_2Cl_2$]$(ClO_4)_2$, which is insoluble both in water and CH_2Cl_2. However, the compound is soluble in nonaqueous polar solvents such as DMF and MeCN. In particular, the absorption spectrum in the UV–vis region superimposes with that measured for the diferrocenium cation anodically generated in MeCN solution (0.1 M in Bu_4NClO_4) in the controlled-potential electrolysis experiment. Thus, the two-phase oxidation by Ce^{IV} in $HClO_4$ represents a quick and convenient method to isolate the oxidized complex. The kinetic stability of the oxidized complex (toward reduction/decomposition) varies with the nature of the solvent, being much higher in MeCN ($t_{1/2}$ = 400 min), than in DMF where the decomposition is almost instantaneous. Thus 100% reduction of the oxidized complex *cis*-[Pt^{II}(3-Fc^+-Py)$_2Cl_2$]$^{2+}$ can be accomplished in MeCN solution using solutions of ascorbic acid and 2,5-di-*tert*-butylhydroquinone. In particular, it is possible to titrate a *cis*-[Pt^{II}(3-Fc^+-Py)$_2Cl_2$]$^{2+}$ solution by the controlled addition of a standard solution of 2,5-di-*tert*-butylhydroquinone.

Conclusions

This work has demonstrated that Pt^{II} behaves as an efficient linking segment to generate bis(ferrocenes). In particular, the *cis*-Py_2Pt^{II} core prevents any electronic interaction between the ferrocene subunits, producing a reducing agent able to release two electrons *in a single shot*. A similar function is performed by the [Py_2Re(CO)$_3$Cl] core, in the [(4-FcPy)$_2$Re(CO)$_3$Cl] complex. It is not clear whether stopping of the electron communication is to be ascribed to the metal center or to the pyridine ligand, to which the Fc moiety is appended, in the 3- or 4-position. In this connection, it is worthwhile noting that in the [(FcPPh$_2$)$_2$Re(CO)$_3$Cl] complex,[4] in which each ferrocene subunit is appended to a phosphine ligand, the two-electron oxidation process takes place according to two quite distinct one-electron steps, whose potentials are separated by 100 mV: this indicates significant coupling of the ferrocene fragments. This would lead us to conclude that, under the appropriate conditions, the metal center (Re, in this case) does not oppose the electron communication and that the stopping effect in the [(4-FcPy)$_2$Re(CO)$_3$Cl] complex (and, presumably, in the *cis*-[Pt^{II}(3-FcPy)$_2Cl_2$] system, too) is exerted by the pyridine ring bridging the metal center and the ferrocene moiety.

Acknowledgment. We thank the Ministry of University, Research and Technology (MURST, Rome) and the National Council of Research (CNR, Rome) for financial support.

Registry No. 2, 97493-87-3; 3, 138490-07-0; Fc, 102-54-5; (3-FcPy)$^+$, 138490-11-6; K_2PtCl_4, 10025-99-7; {*cis*-[Pt(3-FcPy)$_2Cl_2$]}$(ClO_4)_2$, 138490-09-2; *cis*-[Pt(3-FcPy)$_2Cl_2$]$^{2+}$, 138490-08-1; *cis*-[Pt(3-FcPy)$_2Cl_2$]$^+$, 138490-10-5; 3-aminopyridine, 462-08-8; 3-pyridinediazonium, 35332-74-2.

Supplementary Material Available: Listings of positional and isotropic thermal parameters, anisotropic thermal parameters, bond distances, bond angles, and data collection and refinement data (7 pages); a listing of observed and calculated structure factors (38 pages). Ordering information is given on any current masthead page.